Available online at www.sciencedirect.com
SCIENCE DIRECT
Journal of Magnetic Resonance 180 (2006) 127–136
JMR Journal of Magnetic Resonance
www.elsevier.com/locate/jmr

Measurement of one-bond $^{13}C^{\alpha}$–$^{1}H^{\alpha}$ residual dipolar coupling constants in proteins by selective manipulation of $C^{\alpha}H^{\alpha}$ spins

Graeme Ball [a], Nicola Meenan [c,1], Krystyna Bromek [b], Brian O. Smith [b], Juraj Bella [a], Dušan Uhrín [a,*]

[a] School of Chemistry, University of Edinburgh, West Mains Road, Edinburgh EH9 3JJ, UK
[b] Division of Biochemistry and Molecular Biology, Institute Biomedical and Life Sciences, Joseph Black Building, University of Glasgow, Glasgow G12 8QQ, UK
[c] Department of Chemistry, Joseph Black Building, University of Glasgow, Glasgow G12 8QQ, UK

Received 26 October 2005; revised 24 January 2006
Available online 21 February 2006

Abstract

We have developed new 2D and 3D experiments for the measurement of C^{α}–H^{α} residual dipolar coupling constants in ^{13}C and ^{15}N labelled proteins. Two experiments, 2D (HNCO)-(*J*-CA)NH and 3D (HN)CO-(*J*-CA)NH, sample the C^{α}–H^{α} splitting by means of C^{α} magnetization, while 2D (*J*-HACACO)NH and 3D *J*-HA(CACO)NH use H^{α} magnetization to achieve a similar result. In the 2D experiments the coupling evolution is superimposed on the evolution of the ^{15}N chemical shifts and the IPAP principle is used to obtain ^{1}H–^{15}N HSQC-like spectra from which the splitting is determined. The use of a third dimension in 3D experiments reduces spectral overlap to the point where use of an IPAP scheme may not be necessary. The length of the sampling interval in the *J*-dimension of these experiments is dictated solely by the relaxation properties of C^{α} or H^{α} nuclei. This was made possible by the use of C^{α} selective pulses in combination with either a DPFGSE or modified BIRD pulses. Inclusion of these pulse sequence elements in the *J*-evolution periods removes unwanted spin–spin interactions. This allows prolonged sampling periods (~25 ms) yielding higher precision C^{α}–H^{α} splitting determination than is achievable with existing frequency based methods.

Keywords: Protein NMR; BIRD; $^{13}C^{\alpha}$–$^{1}H^{\alpha}$ residual dipolar coupling constants; RDC; DPFGSE

1. Introduction

The introduction of residual dipolar coupling constants (RDCs) as restraints for structure determination by NMR [1,2] made it possible to establish the relative orientation of distant molecular fragments. The angular information derived from RDCs supplements the standard distance and torsional restraints provided by NOEs and scalar couplings and has been shown to improve the accuracy of NMR structures [3,4]. Some of the most commonly measured RDCs in proteins are those between directly bonded nuclei such as N–H, C′–N, C′–C^{α}, and C^{α}–H^{α}. The methodology for the measurement of these coupling constants has advanced considerably during the last eight years [5]. In general, the techniques that have been developed can be grouped into two categories—frequency based methods and intensity [6–9] based methods. As our methods belong to the first category we start with a brief overview of existing techniques from this area.

C^{α}–H^{α} dipolar coupling constants can, in principle, be determined from 2D $^{1}H^{\alpha}$–$^{13}C^{\alpha}$ correlation spectra without heteronuclear decoupling in either of the dimensions while the resulting doubling of spectral lines can be eliminated by spin-state selective filtration [10–12]. The use of these techniques for larger proteins is limited by insufficient

* Corresponding author. Fax: +44 131 650 7155.
E-mail address: dusan.uhrin@ed.ac.uk (D. Uhrín).
[1] Present address: Department of Biology, University of York, P.O. Box 373, York YO10 5YW, UK.

1090-7807/$ - see front matter © 2006 Elsevier Inc. All rights reserved.
doi:10.1016/j.jmr.2006.01.017

resolution of the C^{α}–H^{α} region of ^{13}C–^{1}H HSQC spectra. A potential overlap of H^{α} resonances with the residual H_2O signal limits the use of such techniques to D_2O samples [12]. These problems are eliminated in 3D experiments by incorporating ^{15}N as the third dimension and acquiring amide protons in the directly detected dimension. Such experiments superimpose evolution of the C^{α}–H^{α} couplings on the chemical shift evolution sampled in one of the indirectly detected dimensions. For example, a simple modification of the (HA)CA(CO)NH experiment allows C^{α}-H^{α} couplings to be recorded during a constant time C^{α} chemical shift labelling interval [13]. The length of this interval is set to 28 ms in order to refocus the C^{α}–C^{β} coupling. The same principle is used in a modified (HA)CANH experiment acquired in the $^{1}H^{\alpha}$-coupled mode [14]. For larger proteins, these techniques can suffer from severe signal attenuation due to the fast relaxation of C^{α} spins. This problem is avoided in a 3D (HACA)CONH experiment [15], where the C^{α}–H^{α} couplings are sampled in a variable-time fashion while the magnetization is on H^{α} rather than C^{α} spins. At the same time, the carbonyl chemical shifts are labelled during a 28 ms constant-time interval and antiphase C^{α}–H^{α} doublets are observed in the carbonyl dimension.

In an HNCO-based 3D experiment [16] the evolution of C^{α}–H^{α} couplings is also superimposed on the evolution of carbonyl chemical shifts. The carbonyl chemical shifts are recorded during a semi-constant time period [17,18] and concurrently the C^{α}–H^{α} coupling is sampled while the magnetization is on C^{α}. The length of this variable-time sampling interval must be <12 ms due to the evolution of the C^{α}–C^{β} coupling. To separate individual lines of C^{α}–H^{α} doublets, the authors used the IPAP scheme [19]. The IPAP principle is also employed in another HNCO-based experiment [20]. Here the evolution of C^{α}–H^{α} couplings is superimposed on the evolution of ^{15}N chemical shifts. This sensitivity-enhanced variable-time 2D ^{1}H–^{15}N correlated experiment uses the C'–C^{α} couplings for the IPAP-based separation of spectral lines. The C^{α}–H^{α} splitting is sampled via transverse proton magnetization, thus eliminating the need for constant time C^{α}–C^{β} coupling evolution.

Spin-selective filtration is used in the 3D α/β-HN(CO)CA-*J*-TROSY [21] and 3D HNCA based TROSY experiments [22]. Although these experiments have primarily been designed for the determination of $^{3}J(H^{\alpha},N)$ between H^{α}_{i-1} and N_i [21] and $^{2}D(H^{\alpha},N)$ coupling constants [22], the C^{α}–H^{α} splitting is at the same time obtained from the C^{α} dimension which is sampled in a variable-time fashion. The digital resolution of this dimension is therefore limited due to C^{α}–C^{β} coupling evolution. Another E.COSY based experiment also provides, amongst others, the values of C^{α}–H^{α} splittings [23].

In this work we further explore ways of measuring the C^{α}–H^{α} splittings and present two 2D experiments and two 3D experiments that use selective manipulation of $C^{\alpha}H^{\alpha}$ spins to maximise the definition of C^{α}–H^{α} doublets. These methods utilize C^{α} selective pulses incorporated into a bilinear rotational decoupling (BIRD) pulse [24,25] or a double pulse field gradient spin–echo (DPFGSE) [26]. We show that these modifications remove unwanted interactions and as a consequence increase the precision of the measurements of the C^{α}–H^{α} dipolar coupling constant.

2. Materials and methods

The concentration of ABA-1A used for NMR experiments was 2.5 mM for the isotropic and 1.5 mM for the aligned sample. The protein was dissolved in a solution of 9:1 H_2O/D_2O, 50 mM phosphate buffer (pH 7), and 50 mM NaCl. All spectra were acquired at 37 °C using a 600 MHz Bruker Avance spectrometer equipped with a 5 mm *z*-gradient, triple-resonance cryoprobe. Alignment was achieved using 4.8 mg/ml Pf1 phage [27] (Profos AG, Regensburg, Germany) which gave a residual quadrupolar splitting of D_2O of 13.1 Hz. The following parameters were used for the acquisition of NMR spectra on the aligned sample. The 2D (HNCO)-(*J*-CA)NH spectra (Fig. 2A) were obtained with acquisition times of 107 and 36.8 ms in t_2 and t_1, respectively. A scaling factor $\kappa = 0.667$ was used during the coupling evolution period and 288 scans were accumulated for each of 56 time increments. IP and AP spectra were collected in an interleaved manner giving a total acquisition time of 28.5 h. The 2D (*J*-HACACO)NH spectrum (Fig. 2B) was obtained using acquisition times of 107 ms in t_2 and 36.9 ms in t_1 using a scaling factor $\kappa = 0.667$. 220 scans were accumulated for each of 56 t_1 increments of the interleaved IP and AP spectra giving a total acquisition time of 22 h. The 3D (HN)CO-(*J*-CA)NH spectrum (Fig. 3A) was acquired using acquisition times of 107, 42.1, and 10.6 ms in t_3, t_2 (^{15}N), and t_1 (CO), respectively. A scaling factor $\kappa = 0.667$ was used during the coupling evolution period (t_2) and 16 scans per increment were collected for each of 64 t_2 and 32 t_1 time increments resulting in a total experimental time of 60 h. The 3D *J*-HA(CACO)NH spectrum (Fig. 3B) was acquired using acquisition times of 107, 17.1, and 32.8 ms in t_3, t_2 (^{15}N), and t_1 (H^{α}), respectively. The number of t_1 and t_2 increments were 20 and 48, respectively, and 16 scans were accumulated per increment resulting in a total acquisition time of 54 h. 1D traces shown in Fig. 5 were extracted from the first ^{15}N planes of the 3D *J*-HA(CACO)NH experiments acquired with or without a BIRD pulse using acquisition times of 107 and 32 ms in t_2 and t_1, respectively. Seventy t_1 increments with 144 scans each were acquired in 9.6 h.

All spectra were processed in AZARA (Wayne Boucher, University of Cambridge, http://www.bio.cam.ac.uk/azara), using a Lorentzian to Gaussian window function, fourfold zero filling and Fourier transformation. Linear prediction was not used. In all cases, peak positions were determined using a parabolic interpolation of the maximum in the CCPN analysis program [28]. The signal-to-noise ratios given in captions to Fig. 2 were determined

using BRUKER software with noise regions selected from 4 to 10 ppm of signal-free regions.

3. Results

The proposed experiments use the polarization transfer pathways of existing NMR techniques and we will therefore focus on the new pulse sequence elements rather than describing the new experiments in full. We will start by introducing the experiments that use C^{α} magnetization for the sampling of C^{α}–H^{α} couplings and later describe the experiments that use H^{α} magnetization to achieve a similar result.

3.1. 2D (HNCO)-(J-CA)NH and 3D (HN)CO-(J-CA)NH

The first 2D experiment utilizes the polarization transfer pathway of a 3D HNCO-based scheme [16] and is referred to here as 2D (HNCO)-(*J*-CA)NH (Fig. 1A). In this experiment, carbonyl chemical shifts are not sampled and the C^{α}–H^{α} coupling evolves simultaneously with ^{15}N chemical shifts. Semi-constant time ^{15}N chemical shift labelling is used [17,18] in order to increase the digital resolution in the dimension from which the coupling constants are determined. The 2D (HNCO)-(*J*-CA)NH experiment further differs from the original 3D technique in two ways. First,

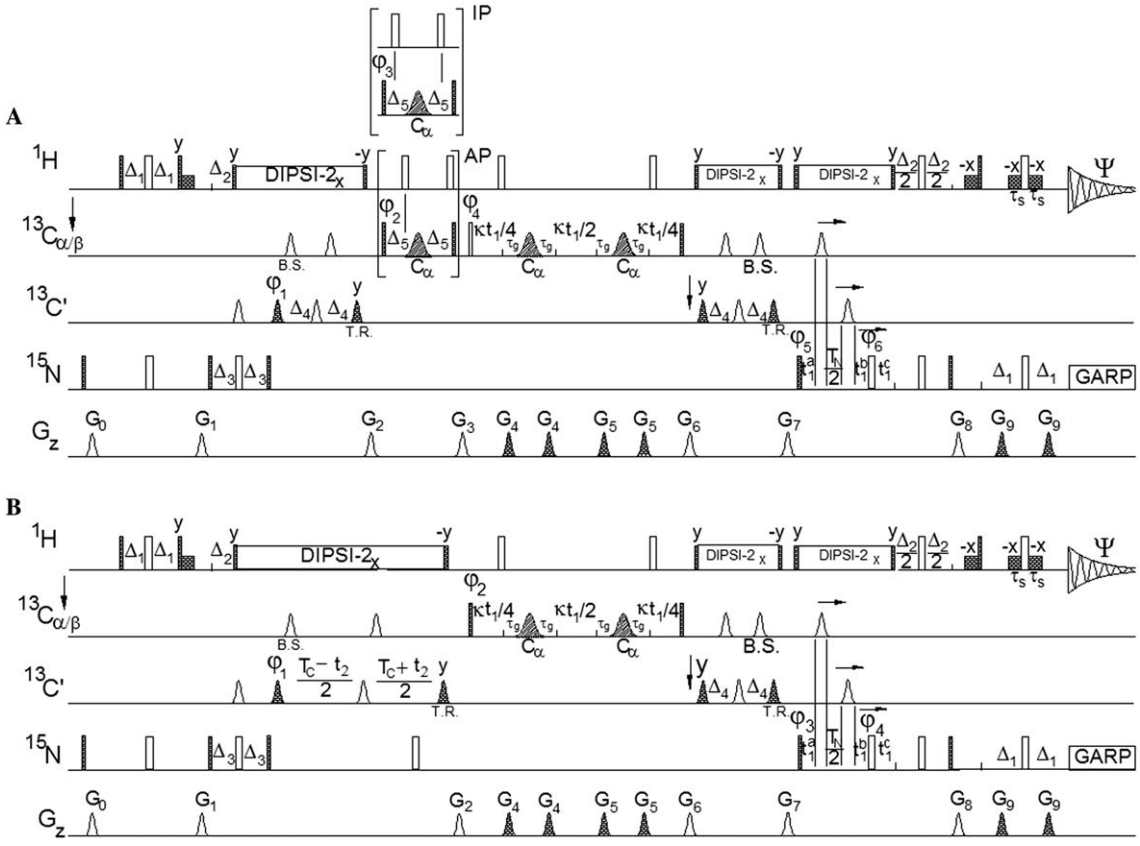

Fig. 1. Pulse sequence of the (A) 2D (HNCO)-(*J*-CA)NH and (B) 3D (HN)CO-(*J*-CA)NH for the measurement of C^{α}–H^{α} coupling constants. Thin filled rectangles represent nonselective 90° ^{1}H or ^{15}N pulses, open wider rectangles are used for nonselective ^{1}H or ^{15}N 180° pulses. Water selective 90° pulses are shown as filled squares. A filled rectangle on the $C^{\alpha/\beta}$ line represents a rectangular 90° ^{13}C pulse, the duration of which is calculated to be $\sqrt{15}/4\Delta$, where Δ is the separation in Hz between the $^{13}C'$ and $^{13}C^{\alpha}$ offsets [37]. The 90° ^{13}C selective Q5 pulses are 320 μs long and are represented by filled Gaussian shapes. Time reversed pulses are marked T.R. The 180° ^{13}C selective Q3 pulses are 256 μs long and are shown as open Gaussian shapes. Bloch–Siegert shift compensating pulses are denoted B.S. The 1.4 ms C^{α} selective 180° Q3 pulses (600 MHz) are applied at 58 ppm and are drawn as shaded Gaussian pulses with a C^{α} symbol. Unless stated otherwise, pulses are applied from the *x* axis. The sine shaped pulsed field gradients were 1ms (open Gaussian) or 0.5 ms (filled Gaussian) in length. The ^{13}C carrier frequency was changed at the points indicated by vertical arrows (176 ppm for CO and 58 ppm for C^{α}). The following parameters were used: $\tau_g = 0.5$ ms, $\Delta_1 = 2.3$ ms, $\Delta_2 = 5.3$ ms, $\Delta_3 = 12.3$ ms, $\Delta_4 = 4.0$ ms, $\Delta_5 = 1.78$ ms, $T_N = 24.8$ ms, $T_C = 11.0$ ms, $\tau_S = 1.4$ ms. For the semi-constant time ^{15}N frequency labelling period t_1, where $T_N/2 = 12.4$ ms, AT is the total acquisition time, *n* is the number of t_1 points and *i* is the index of each point then $t_{1a} = (AT/2)\cdot(i/(n-1))$, $t_{1b} = ((AT - T_N)/2)\cdot(i/(n-1))$ and $t_{1c} = (T_N/2) - (T_N/2)\cdot(i/(n-1))$. The following phase cycling was used in (A) $\varphi_1 = 8(x), 8(-x)$; $\varphi_2 = 2(y), 2(-y)$; $\varphi_3 = 2(x), 2(-x)$, $\varphi_6 = 16(x), 16(-x)$ and $\Psi = x, 2(-x), x, -x, 2(x), -x$. Phases φ_5 and φ_6 were incremented according to the States-TPPI protocol in order to achieve sign discrimination in the indirectly detected dimension. For IP spectra $\varphi_4 = x, -x$ and $\varphi_5 = 4(x), 4(-x)$; while for the AP spectra $\varphi_4 = y, -y$ and $\varphi_3 = 4y, 4(-y)$. The phase cycling used in (B) was $\varphi_1 = 2x, 2(-x)$; $\varphi_2 = x, -x$; $\varphi_3 = 4(x), 4(-x)$, $\varphi_4 = 8(x), 8(-x)$ and $\Psi = x, 2(-x), x, -x, 2(x), -x$. Phases φ_1 (t_2) and φ_3 and φ_4 (t_1) were incremented according to the States-TPPI protocol in order to achieve sign discrimination in the indirectly detected dimensions. *z*-Gradient strengths for schemes (A) and (B), expressed as a percentage of the maximum strength available (50 Gauss/cm), were $G_0 = 15$, $G_1 = 50$, $G_2 = 10$, $G_3 = 30$, $G_4 = 12$, $G_5 = 17$, $G_6 = 8$, $G_7 = 40$, $G_8 = 60$, and $G_9 = 60$.

spin-state selection prior to the C^{α}–H^{α} evolution period is achieved by a modification of the IPAP scheme proposed by Permi et al. [29]. By using a 180° C^{α} selective pulse instead of a $C^{\alpha/\beta}$ selective pulse, C^{α}–C^{β} couplings are refocused by the end of the IPAP spin–echo, which increases the signal intensity by 8% compared to a filter where both the C^{α} and C^{β} carbons are inverted. The second, more significant modification, involves application of a C^{α} selective 180° pulse during the variable-time coupling constant sampling period, t_1. This modification allows extension of the sampling interval beyond ~12 ms since the C^{α}–C^{β} coupling is refocused at the end of the t_1 period. The arrangement of the C^{α} selective pulses within a DPFGSE is crucial to obtaining pure in-phase or antiphase C^{α}–H^{α} doublets during the coupling evolution period. We have found that some peaks showed phase distortions when a single pulsed field gradient spin–echo was used for this purpose. This would compromise accurate determination of coupling constants. Evolution of heteronuclear couplings during the pulsed field gradients of the DPFGSE is eliminated by two 180° ^{1}H pulses applied before and after the first and the second C^{α} selective 180° pulse, respectively. Asymmetric arrangement of 180° ^{1}H pulses, e.g., both applied after the C^{α} selective 180° pulses, was found also to lead to phase distortions. At 600 MHz we typically use 1.4 ms Q3 pulses [30] centred at 58 ppm to achieve selective inversion of C^{α} spins. In addition to inverting C^{α} carbons, these pulses also invert the C^{β} resonances of serines and threonines so that the C^{α}–H^{α} doublets of these residues are further modulated by C^{α}–C^{β} coupling constants. Glycine C^{α} resonances, on the other hand, are not inverted at all and their magnetization is dephased by PFGs. For glycine only the sum of the two coupling constants of the CH_2 group could be obtained by this and similar methods even if the glycine C^{α} were inverted. All the remaining 17 amino acids have their C^{α} resonances sufficiently resolved from their C^{β} resonances[2] to fully benefit from this modification. To minimize loss of magnetization due to the relatively fast relaxation of C^{α} it is possible to scale down evolution of the coupling constants by an arbitrary factor κ, as shown previously [16].

We illustrate our methods using a 15 kDa mostly α-helical protein, ABA-1A, from *Ascaris suum* with rotation correlation time, $\tau_c = 7.1$ ns. Partial, edited 2D IPAP (HNCO)-(*J*-CA)NH spectra (Fig. 2A) acquired with an aligned sample show a good separation of the two lines of the C^{α}–H^{α} doublet. Clearly, the crowded nature of the ^{1}H–^{15}N HSQC spectrum for this α-helical protein meant that without the extended ^{15}N acquisition times used here, the resolution would not have been sufficient for determination of the coupling constants. The signals that were weaker than the average had lower intensity in the spectra of both the isotropic (data not shown) and aligned samples, indicating that relaxation effects along the polarization transfer pathway, rather than the effects of alignment, were responsible for signal loss. The central region of this ^{1}H–^{15}N correlation map is still very crowded. As shown by Yang et al. [16] introduction of a third dimension helps to alleviate these problems.

A constant-time carbonyl chemical shift labelling (t_2) can easily be reinstated in place of the first $2\Delta_4$ interval of the (HNCO)-(*J*-CA)NH experiment creating a new 3D (HN)CO-(*J*-CA)NH experiment (Fig. 1B). Unlike the experiment of Yang et al. [16], the C^{α}–H^{α} evolution in this 3D experiment is concurrent with the ^{15}N chemical shift labelling period and not with that of the carbonyls. We find that a rather short carbonyl chemical shift evolution period efficiently resolves much of the overlap observed in the 2D ^{15}N–^{1}H HSQC-like spectra and that, at the same time, the IPAP procedure is not required for this 3D experiment. Baseline resolution of in-phase C^{α}–H^{α} doublets is achieved by the use of semi constant time ^{15}N chemical shift labelling and a longer sampling period made possible by the use of the C^{α} selective DPFGSE. The removal of the IPAP element increases the sensitivity of the measurements, particularly for aligned samples showing a large spread of splittings. A representative 2D ^{1}H–^{15}N plane from a 3D (HN)CO-(*J*-CA)NH spectrum acquired from the aligned sample illustrates this increased resolution (Fig. 3A).

3.2. 3D *J*-HA(CACO)NH and 2D (*J*-HACACO)NH

In the two experiments discussed next, the C^{α}–H^{α} coupling constants are obtained by modulating the H^{α} magnetization rather than that of C^{α}. This time we introduce the 3D experiment first. In the experiment referred to here as 3D *J*-HA(CACO)NH (Fig. 4A), the H^{α} chemical shifts together with the C^{α}–H^{α} couplings are sampled during a variable-time t_1 acquisition period. The magnetization is then transferred via carbonyl carbons to nitrogen atoms for ^{15}N chemical shift labelling (constant time, t_2) and is eventually detected on NH protons (t_3). The C^{α}–H^{α} splittings are extracted from the H^{α} dimension of ^{15}N planes where they appear as antiphase doublets. The key to the improved sampling of C^{α}–H^{α} couplings in comparison with other experiments that use modulation of H^{α} coherences [15,20] is the removal of unnecessary interactions of H^{α} protons, in particular their dipole–dipole interactions with other protons. Along similar lines, the Lee–Goldburgh decoupling of homonuclear dipolar couplings, was shown to remove the truncation of the signal allowing the measurement of long-range residual dipolar coupling constants in proteins [31]. To achieve a similar effect here, we use modified BIRD pulses [25]. Such pulses have been used previously to remove unwanted interaction from the indirectly detected dimensions of 2D experiments [32,33]. The modified BIRD pulse applied in the middle of the t_1 period eliminates evolution of proton–proton couplings that would otherwise accelerate signal decay. Such effects can be observed in isotropic samples where each H^{α} proton is coupled to one NH and one or two H^{β} protons, but more

[2] http://www.bmrb.wisc.edu/search/stats_diamagnetic.html.

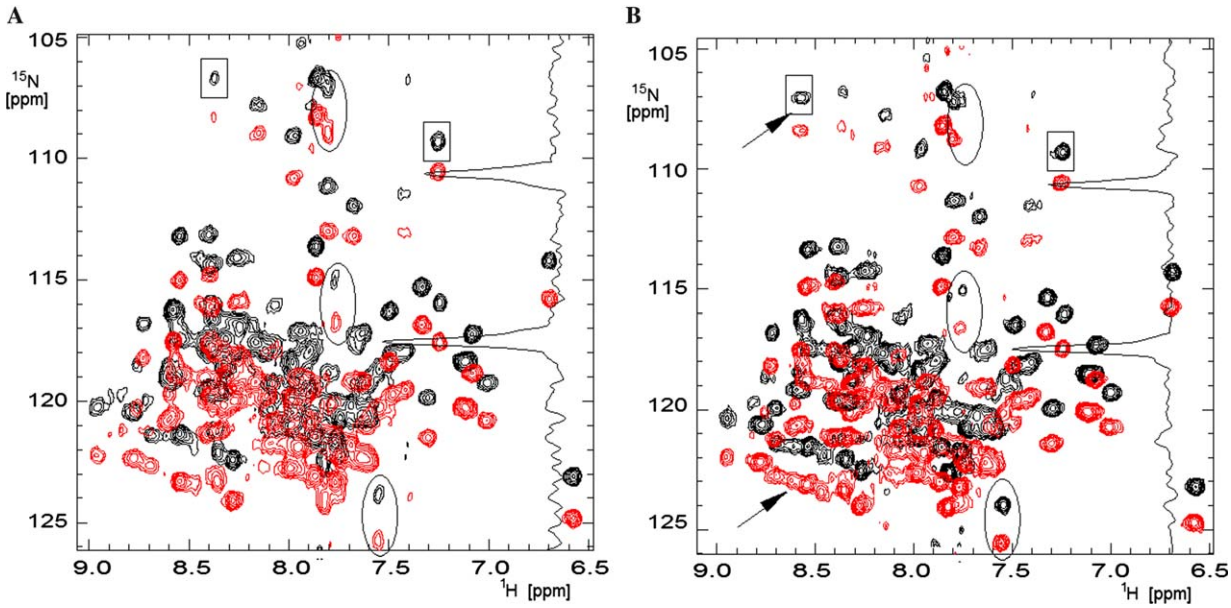

Fig. 2. Overlay of IPAP edited spectra acquired using (A) the 2D (HNCO)-(*J*-CA)NH (Fig. 1A) pulse sequence, and (B) the 2D (*J*-HACACO)NH pulse sequence (Fig. 4B) on the aligned sample of ABA-1A. Circled signals correspond to residues preceded by serines or threonines; signals that are stronger in spectrum (B) are indicated by arrows. The signal-to-noise ratios (SNR) for the two boxed peaks were 8:1 and 13:1 in spectrum (A) and 15:1 and 18:1 in spectrum (B), respectively. The SNR in spectra acquired using the unaligned protein (data not shown) were 2–3 times higher. For parameters see Section 2.

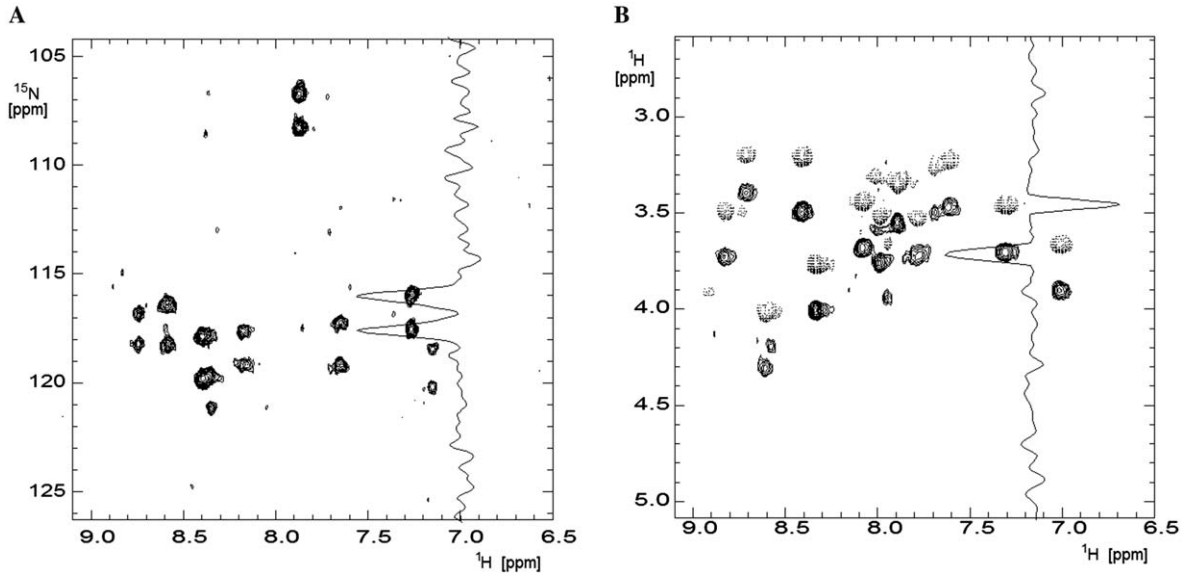

Fig. 3. (A) A representative carbonyl plane from the 3D (HN)CO-(*J*-CA)NH spectrum of the aligned sample of ABA-1A acquired using the pulse sequence shown in Fig. 1B. The scaled C^{α}–H^{α} splittings show as in-phase doublets along the ^{15}N dimension. (B) A representative nitrogen plane from the 3D *J*-HA(CACO)NH spectrum of the aligned sample of ABA-1A acquired using the pulse sequence in Fig. 4A. The C^{α}–H^{α} couplings show as antiphase doublets along the H^{α} dimension. Negative cross peaks were drawn using dotted lines. A F_1 trace through NH proton at 7.3 ppm is shown in both spectra. For parameters Section 2.

significantly, in aligned samples where numerous proton–proton dipolar interactions arise. BIRD pulses were originally designed for selective inversion of protons attached either to ^{13}C or ^{12}C atoms [24]. When applied to compounds with a natural abundance of ^{13}C, BIRD pulses can therefore be used for refocusing proton–proton interactions between these two types of protons. The same effect in fully ^{13}C-labelled proteins can still be achieved providing only certain carbon resonances are inverted by the BIRD pulse. When a selective pulse is used in place of the central nonselective carbon pulse of the BIRD pulse, protons attached to carbons that are not inverted behave as if they were attached to ^{12}C atoms. As pointed out above, the C^{α} carbons of proteins (except those of threonine and serine

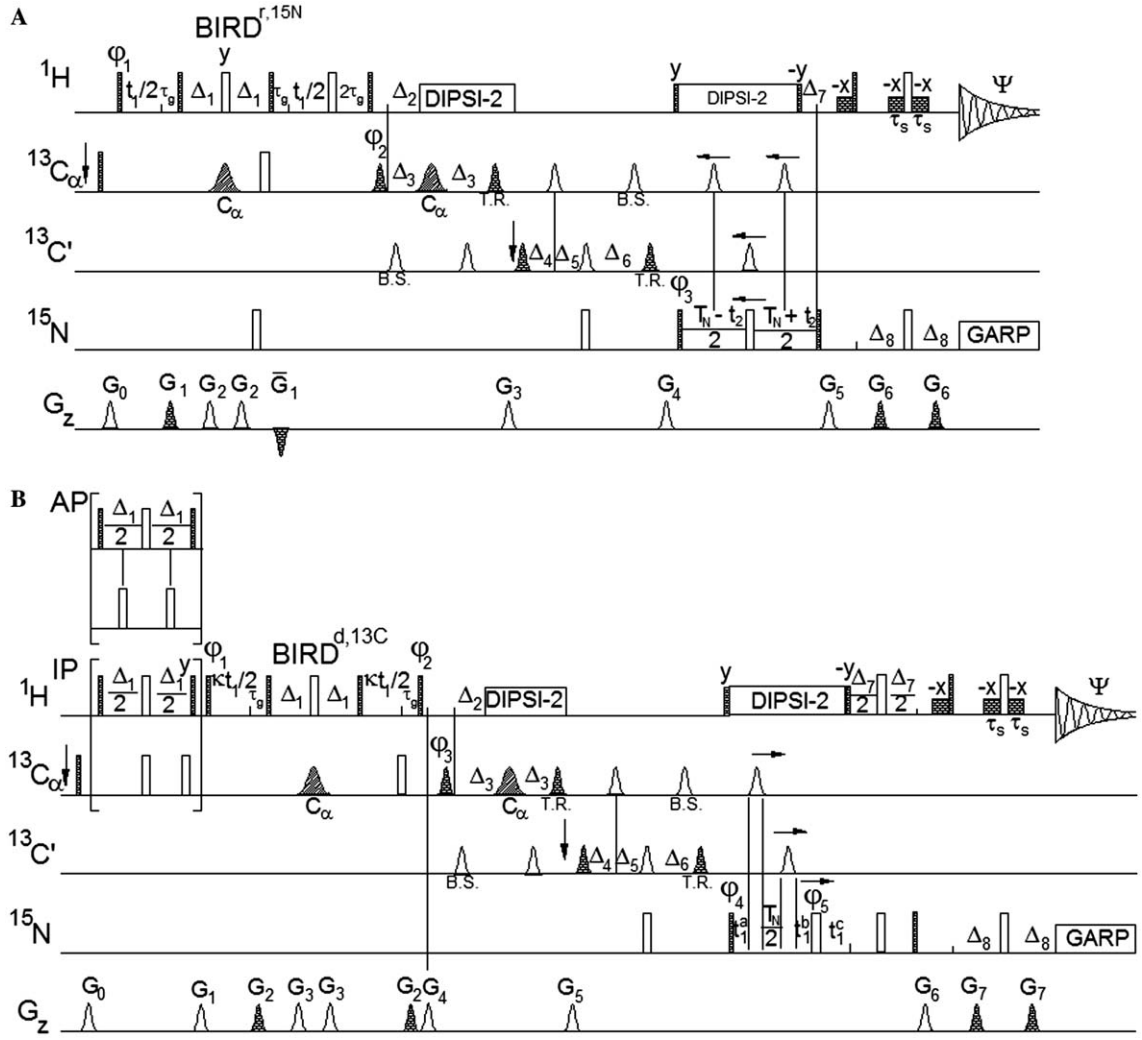

Fig. 4. Pulse sequences for the measurement of C^{α}–H^{α} coupling constants: (A) 3D *J*-HA(CACO)NH and (B) 2D (*J*-HACACO)NH. The meaning of symbols is explained in the caption to Fig. 1. The following parameters were used for pulse sequence (A): $\tau_g = 0.5$ ms, $\Delta_1 = 3.57$ ms, $\Delta_2 = 3.57$ ms (1.79 ms for glycine residues), $\Delta_3 = 3.75$ ms, $\Delta_4 = 4.5$ ms, $\Delta_5 = 7.9$ ms, $\Delta_6 = 12.4$ ms, $T_N = 24.8$ ms, $\Delta_7 = 5.3$ ms, $\Delta_8 = 2.3$ ms, $\tau_S = 1.4$ ms. Values of t_{1a}, t_{1b} and t_{1c} for the t_1 semi-constant time ^{15}N frequency labelling period are identical to those used in the 2D (HNCO)-(*J*-CA)NH experiment shown in Fig. 1. The following phase cycling was used in (a): $\varphi_1 = x, -x$; $\varphi_2 = 4(x), 4(-x)$; $\varphi_3 = 2(x), 2(-x)$ and $\Psi = x, 2(-x), x, -x, 2(x), -x$. Phases φ_1 and φ_3 were incremented according to the States-TPPI protocol in order to achieve sign discrimination in the indirectly detected dimensions. For pulse sequence (B) the following phase cycling was used: $\varphi_1 = 4(x), 4(-x)$; $\varphi_3 = x, -x$; $\varphi_5 = 8(x), 8(-x)$; and $\Psi = x, 2(-x), x, -x, 2(x), -x$. For IP part $\varphi_2 = x$ and $\varphi_4 = 2(x), 2(-x)$; while for the AP part $\varphi_2 = y$ and $\varphi_4 = 2(y), 2(-y)$. Phases φ_4 and φ_5 were incremented according to the States-TPPI protocol. *z*-Gradient strengths for scheme (A), expressed as a percentage of the maximum (50 Gauss/cm), were $G_0 = 8$, $G_1 = 9$, $G_1 = -9$, $G_2 = 14$, $G_3 = 50$, $G_4 = 60$, $G_5 = 60$, and $G_6 = 60\%$ and for scheme (B), $G_0 = 8$, $G_1 = 30$, $G_2 = 12$, $G_3 = 17$, $G_4 = 32$, $G_5 = 40$, $G_6 = 50$, and $G_7 = 70\%$.

residues) can easily be selectively inverted. In the 3D *J*-HA(CACO)NH experiment H^{α} chemical shifts are sampled together with C^{α}–H^{α} couplings, which means that neither H^{α} nor C^{α} spins must be inverted during the t_1 period. To achieve this we use a modified $BIRD^{r}$ pulse [25] with the central 180° carbon pulse substituted by a C^{α} selective pulse. Additionally, to refocus any dipolar H^{α}–^{15}N interactions, a 180° ^{15}N pulse can be applied together with the final ^{13}C nonselective pulse of such a C^{α}-$BIRD^{r,15N}$ pulse.

The overall effect of the C^{α}-$BIRD^{r,15N}$ pulse, applied in the middle of the t_1 period is summarized in Table 1. As a consequence all proton–proton interactions of H^{α} (with the

Table 1
Effects of C^{α}-$BIRD^{r,15N}$ and C^{α}-$BIRD^{d,13C}$ pulses

X	C^{α}-$BIRD^{r,15N}$	C^{α}-$BIRD^{d,13C}$
$^{13}C^{\alpha}$	0/Yes	180/Yes
C^{other}	180/No	0/No
$^{1}H^{\alpha}$	0/Yes	180/Yes
H^{other}	180/No	0/No
^{15}N	180/No	0/No

0 or 180 indicates the flip angle experienced by spin X as a consequence of the appropriate C^{α}-BIRD pulse; Yes or No indicates whether the X-H^{α} coupling is active during a spin–echo with central C^{α}-BIRD pulse. r, remote protons, or "effectively" attached to ^{12}C; d, protons directly attached to ^{13}C, C^{other} are non-$^{13}C^{\alpha}$ carbons, H^{other} are non-$^{1}H^{\alpha}$ protons.

exception of dipolar interactions with other H^{α} protons) are refocused as well as their long-range heteronuclear interactions (with the exception of dipolar interactions with other C^{α} carbons). Since H^{α} protons are not inverted by C^{α}-BIRD^{r,15N}, a pair of gradients with opposite polarity and duration τ_g is inserted on either side of the C^{α}-BIRD^{r,15N} pulse. The chemical shift and heteronuclear coupling evolution of H^{α} protons during the pulsed field gradients are eliminated by a 180° ^{1}H pulse at the end of the t_1 period followed by a delay of $2\tau_g$. Another pair of PFGs were placed inside the BIRD pulse. When this pulse sequence element was incorporated into a standard ^{1}H–^{13}C HSQC experiment and tested on a ^{13}C-1 labelled glucose sample, pure phase antiphase doublets were obtained for Δ_1 ($= 1/2\ ^1J_{CH}$) delays calculated using a range of $^1J_{CH}$ values. Variation of the one-bond heteronuclear splittings, or nonideal 180° pulses only decrease the signal intensity without modulating the magnetization [34]. This was confirmed in a series of experiments where the offset of the 180° C^{α} selective pulse was varied.

The effects of the C^{α}-BIRD^{r,15N} pulse are illustrated in Fig. 5 in the context of the 3D *J*-HA(CACO)NH experiment without and with the C^{α}-BIRD^{r,15N} pulse using an aligned sample of ABA-1A. It is evident that the magnetization decayed typically 10–25% less from the comparison of traces extracted from these experiments. The use of C^{α}-BIRD^{r,15N} pulse results in narrower lines, providing a better definition of the splittings. These lines are also more intense despite significant deviations of the actual splittings from those used to calculate the Δ_1 delay.

An advantage of the 3D *J*-HA(CACO)NH experiment compared to the ^{13}C sampled methods are that, in principle, two C^{α}–H^{α} coupling constants can be determined for glycine corresponding to its two nonequivalent H_{α} protons. In this case, the C^{α} resonances of glycine must also be inverted, e.g., by using an 1 ms Q3 pulse centred at 55 ppm. This change must be accompanied by a shortening of the refocusing delay Δ_2 from $1/2^1J_{CH}$ to $1/4^1J_{CH}$. The sensitivity of such an experiment is therefore lower (data not shown). Please note that the evolution of the geminal homonuclear coupling constant of the CH_2 group of glycine is not refocused by the modified BIRD pulse and can, especially in the aligned sample, contribute to broadening of spectral lines.

One other aspect of the proposed pulse sequence deserves a short discussion. After the transfer of magnetization to C^{α} carbons, evolution occurs to produce antiphase magnetization with respect to carbonyl carbons. When both C^{α} and C^{β} together with C′ carbons are inverted midway through this interval, a maximum transfer efficiency of 0.46 is achieved for $\Delta_3 = 5$ ms, assuming $J_{C\alpha,C\beta} = 55$ Hz, $J_{C\alpha,C\beta} = 35$ Hz and $T_{2C\alpha} = 30$ ms. This is increased to 0.75 (or by 63%) when the Δ_3 is set to 7.5 ms and the C^{β} carbons are not inverted due to the use of the C^{α} selective pulse. This gain will not apply to serine and threonine as their C^{β} resonances will also be inverted. For the same reason, evolution of H_{α}–H_{β} couplings during the t_1 period is not removed for these residues. Scaling down of the C^{α}–H^{α} splittings is not possible in this 3D experiment since these are sampled together with the H^{α} chemical shifts.

Fig. 3B shows a representative 2D plane from the full 3D experiment, 3D *J*-HA(CACO)NH spectrum acquired using the aligned sample of ABA-1A. As can be seen, the digital resolution obtained in the H^{α} dimension of this 3D experiment is sufficient to resolve individual C^{α}–H^{α} couplings, which appear as antiphase doublets along the H^{α} axis of the ^{15}N planes. If required, the IPAP element could replace the initial 90° ^{1}H of this pulse sequence as illustrated next on a related 2D experiment.

The 3D *J*-HA(CACO)NH experiment can easily be converted to a 2D experiment in which one-bond C^{α}–H^{α} couplings evolve concurrently with ^{15}N chemical shifts.

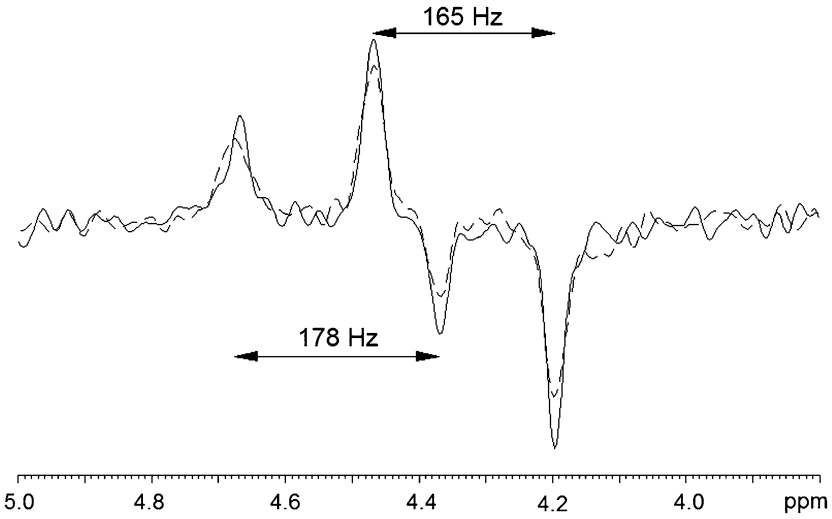

Fig. 5. The effect of the C^{α}-BIRD^{r,15N} pulse. 1D traces parallel to the H_{α} dimension obtained from the first ^{15}N planes of 3D *J*-HA(CACO)NH experiments acquired with (full line) or without (dashed line) a C_{α}-BIRD^{r,15N} pulse. The antiphase doublets corresponding to the H^{α}–C^{α} splittings of two residues with identical NH chemical shifts are shown. For parameters see Section 2.

The pulse sequence for such a 2D (*J*-HACACO)NH experiment is shown in Fig. 4B. As proton chemical shifts are not recorded during the t_1 period of this 2D experiment H^α spins must be inverted. Therefore, C^α spins must also be inverted in order to preserve the evolution of C^α–H^α couplings. This is achieved by a C^α-$BIRD^{d,13C}$ pulse, which shows the same effective spin–spin interaction for H^α protons as does the C^α-$BIRD^{r,15N}$ pulse (Table 1). A pair of PFGs of equal polarity is placed at the end of the $t_1/2$ interval and prior to the polarization transfer to C^α. A 180° ^{13}C pulse applied at the end of the t_1 period removes coupling evolution during the PFGs. Replacing the constant time ^{15}N chemical shift labelling period of the 3D experiment with a semi-constant time interval increases the digital resolution in the ^{15}N dimension from which the coupling constants are to be determined. Scaling down the effective coupling evolution is possible in this 2D experiment. A partial 2D (*J*-HACACO)NH spectrum of aligned ABA-1A is shown in Fig. 2B. As can be seen by comparison with the spectrum acquired using the 2D (HNCO)-(*J*-CA)NH experiment (Fig. 2A), both methods yield spectra of comparable quality, although some cross peaks, indicated by arrows, are more intense in the 2D (*J*-HACACO)NH spectrum. Cross peaks showing the C^α–H^α splittings of threonines and serines in the latter spectrum are not modulated by the C^α–C^β coupling constant and are therefore more intense.

4. Discussion

There are two reasons to suppose that the precision of the coupling constant determination in frequency based methods should improve when using extended sampling periods and removing all but the one splitting of interest. First, longer acquisition times lead to higher primary digital resolution thus improving the definition of peak frequencies. This cannot be substituted by zero-filling: zero-filling beyond one acquisition time only interpolates between points [35]. The only reason why two- or even fourfold zero filling is a common practice is that some peak picking algorithms have been shown to perform more reliably when extended zero filling is used [36]. The second reason has to do with the accuracy with which the peak picking can be performed. Kontaxis et al. [36] have also shown that the random error of peak picking increases relatively rapidly with increasing decay rates, reflecting the increase in the linewidths.

Our experiments address both points: by removing unnecessary interactions we obtain narrower spectral lines (see Fig. 5) and consequently allow longer acquisition times to be used. For example when C^α magnetization is evolving under the effect of C^α–C^β couplings it decays effectively completely by around 14 ms [16]. This decay causes a significant additional line broadening. On the other hand our C^α selective DPFGSE used in the 2D (HNCO)-(*J*-CA)NH and 3D (HN)CO-(*J*-CA)NH experiments removes the C^α–C^β interactions, permitting longer sampling periods. Indeed, a comparison of the of C^α–H^α coupling constants determined from three repeats of 2D (HNCO)-(*J*-CA)NH experiments acquired either with or without the DPFGSE during t_1 showed a 50% reduction in rmsd from 1.3 to 0.6 Hz. These experiments, performed on an unaligned sample of a 15 kDa protein used t_1 acquisition times of 36.8 and 17.5 ms which correspond to coupling evolution times of 24.5 and 11.7 ms ($\kappa = 0.667$), respectively.

No additional advantage was found in extending the coupling evolution period beyond 24 ms—for a dataset with an acquisition time of 69.9 ms in the indirect dimension (46.6 ms coupling evolution time) an rmsd of 1.1 Hz was obtained. This is because of the progressively worsening signal-to-noise ratio (SNR) arising from later FIDs due to the relaxation of C^α coherences. This highlights the importance of a good SNR for reliable peak picking: it is our experience that the beneficial effects of extended sampling periods are lost when the final SNR drops below 10:1. In such cases it is advisable to accumulate more scans into fewer increments.

When performing this comparison we also established that the use of a longer sampling period (24.5 ms) together with the implementation of a semi constant time ^{15}N chemical shift labelling period lead to improved resolution of 2D spectra allowing more coupling constants to be extracted than from spectra acquired using an 11.7 ms evolution time.

Our results (0.6 Hz rmsd for C^α–H^α couplings for a 15 kDa protein) provide a basis for comparison of our methods with those already published. Yang et al. [16] have observed an rmsd of 1.3 Hz for C^α–H^α coupling constants determined from ubiquitin (8.5 kDa) in an experiment that is analogous to our 2D (HNCO)-(*J*-CA)NH without the DPFGSE, while much higher precision (rmsd $\pm$ 0.06 Hz) was achieved from a ubiquitin sample using an intensity based experiment [9]. It is very likely that such a level of precision would not be achievable for larger proteins using the intensity based method due to limiting C^α relaxation during the 28 ms constant time interval. A thorough comparison of the performance of various frequency and intensity based methods for the measurement of C^α–H^α coupling constants is beyond the scope of this paper as it depends on many factors, including protein, concentration, efficiency of polarization transfer pathways, manner of sampling, etc.

The C^α–H^α splittings measured using the 2D and two 3D methods presented in this paper were compared using an aligned sample of ABA-1A. Conservative sets of between 33 and 47 splittings originating from overlap free resonances were chosen for these comparisons. Their values varied between 110 and 190 Hz. Altogether, six pairs of spectra were compared and pairwise rmsd values of 1.7–2.3 Hz (average 2.0 Hz) were observed between C^α–H^α splittings. No systematic differences between any of the sets were observed indicating that none of the methods introduced any systematic errors.

All published experiments for the measurement of C^α–H^α coupling constants in which ^{15}N nuclei are involved

use extended polarization transfer pathways, typically applied in 3D experiments. As a consequence, these experiments are much more prone to relaxation related losses and less sensitive than, for example, those for the measurement of NH coupling constants. Our experiments are no exception. A useful measure of their sensitivity, which can easily be obtained, is the comparison of the signal intensity relative to ^{15}N–^{1}H HSQC spectra. For our 15 kDa ABA-1A sample we obtained relative intensities of 0.19 and 0.16 for 2D (*J*-HACACO)NH and 2D (HNCO)-(*J*-CA)NH, respectively. Similar data for the CT experiment using a 8, 16, and 18 kDa proteins were given as 0.25, 0.15, and 0.10, respectively [9]. These data indicate why longer spectrometer times are required for the measurement of $H^{\alpha}C^{\alpha}$ coupling constants.

5. Conclusions

We have presented two frequency based 2D and two 3D experiments for the measurement of H^{α}–C^{α} residual dipolar coupling constants and demonstrated that these methods increase the precision of the coupling constant determination compared with previously published methods. This is a consequence of using prolonged sampling periods (~25 ms). This was made possible by the use of a C^{α} selective DPFGSE or a modified BIRD pulse which remove undesirable interactions with other spins. These modifications in combination with semi constant-time ^{15}N chemical shift labelling resulted in improved resolution of the ^{1}H–^{15}N correlation maps allowing more coupling constants to be determined. The sensitivity of these experiments was also improved compared against previously published frequency based methods that utilize similar polarization transfer pathways. These experiments are aimed at medium size proteins (12–25 kDa), where the benefits of longer sampling periods can be realized. For smaller proteins, constant time experiments may offer higher precision, while the very fast relaxation of C^{α} resonances in larger proteins prohibits the use of prolonged sampling periods.

References

[1] J.R. Tolman, J.M. Flanagan, M.A. Kennedy, J.H. Prestegard, Nuclear magnetic dipole interactions in field-oriented proteins: information for structure determination in solution, Proc. Natl. Acad. Sci. USA 92 (1995) 9279–9283.

[2] N. Tjandra, A. Bax, Direct measurement of distances and angles in biomolecules by NMR in a dilute liquid crystalline medium, Science 278 (1997) 1111–1114.

[3] G.M. Clore, M.R. Starich, C.A. Bewley, M.L. Cai, J. Kuszewski, Impact of residual dipolar couplings on the accuracy of NMR structures determined from a minimal number of NOE restraints, J. Am. Chem. Soc. 121 (1999) 6513–6514.

[4] A. Bax, G. Kontaxis, N. Tjandra, Dipolar couplings in macromolecular structure determination, Methods Enzymol. 339 (2001) 127–174.

[5] J.H. Prestegard, C.M. Bougault, A.I. Kishore, Residual dipolar couplings in structure determination of biomolecules, Chem. Rev. 104 (2004) 3519–3540.

[6] N. Tjandra, S. Grzesiek, A. Bax, Magnetic field dependence of nitrogen-proton *J* splittings in ^{15}N-enriched human ubiquitin resulting from relaxation interference and residual dipolar coupling, J. Am. Chem. Soc. 118 (1996) 6264–6272.

[7] N. Tjandra, A. Bax, Measurement of dipolar contributions to $^{1}J_{CH}$ splittings from magnetic-field dependence of *J* modulation in two-dimensional NMR spectra, J. Magn. Reson. 124 (1997) 512–515.

[8] T.K. Hitchens, S.A. McCallum, G.S. Rule, A J^{CH}-modulated 2D (HACACO)NH pulse scheme for quantitative measurement of $^{13}C^{\alpha}$–$^{1}H^{\alpha}$ couplings in ^{15}N, ^{13}C-labeled proteins, J. Magn. Reson. 140 (1999) 281–284.

[9] R.L. McFeeters, C.A. Fowler, V.V. Gaponenko, R.A. Byrd, Efficient and precise measurement of H^{α}–C^{α}, C^{α}–C'^{α}, C^{α}–C^{β} and H^{N}–N residual dipolar couplings from 2D H^{N}–N correlation spectra, J. Biomol. NMR 31 (2005) 35–47.

[10] P. Andersson, K. Nordstrand, M. Sunnerhagen, E. Liepinsh, I. Turovskis, G. Otting, Heteronuclear correlation experiments for the determination of one-bond coupling constants, J. Biomol. NMR 11 (1998) 445–450.

[11] P. Andersson, J. Weigelt, G. Otting, Spin-state selection filters for the measurement of heteronuclear one-bond coupling constants, J. Biomol. NMR 12 (1998) 435–441.

[12] P. Wurtz, K. Fredriksson, P. Permi, A set of HA-detected experiments for measuring scalar and residual dipolar couplings, J. Biomol. NMR 31 (2005) 321–330.

[13] M. Ottiger, A. Bax, Determination of relative N–H^{N}, N–C′, C^{α}–C′, and C^{α}–H^{α} effective bond lengths in a protein by NMR in a dilute liquid crystalline phase, J. Am. Chem. Soc. 120 (1998) 12334–12341.

[14] M. Zweckstetter, A. Bax, A single-step determination of protein substructures using dipolar couplings: aid to structural genomics, J. Am. Chem. Soc. 123 (2001) 9490–9491.

[15] W. Hu, Z. Zhang, Y.A. Chen, A high sensitivity 3D experiment for measuring C^{α}–H^{α} residual dipolar coupling constants, J. Magn. Reson. 165 (2003) 248–252.

[16] D. Yang, J.R. Tolman, N.K. Goto, L.E. Kay, An HNCO-based pulse scheme for the measurement of $^{13}C^{\alpha}$–$^{1}H^{\alpha}$ one-bond dipolar couplings in ^{15}N, ^{13}C labeled proteins, J. Biomol. NMR 12 (1998) 325–332.

[17] S. Grzesiek, A. Bax, Amino acid type determination in the sequential assignment procedure of uniformly $^{13}C/^{15}N$-enriched proteins, J. Biomol. NMR 3 (1993) 185–204.

[18] T.M. Logan, E.T. Olejniczak, R.X. Xu, S.W. Fesik, A general method for assigning NMR spectra of denatured proteins using 3D HC(CO)NH-TOCSY triple resonance experiments, J. Biomol. NMR 3 (1993) 225–231.

[19] M. Ottiger, F. Delaglio, A. Bax, Measurement of *J* and dipolar couplings from simplified two-dimensional NMR spectra, J. Magn. Reson. 131 (1998) 373–378.

[20] K. Ding, A.M. Gronenborn, Sensitivity-enhanced IPAP experiments for measuring one-bond $^{13}C'$–$^{13}C^{\alpha}$ and $^{13}C^{\alpha}$–$^{1}H^{\alpha}$ residual dipolar couplings in proteins, J. Magn. Reson. 167 (2004) 253–258.

[21] P. Permi, I. Kilpeläinen, A. Annila, Determination of backbone angle ψ in proteins using a TROSY-based α/β-HN(CO)CA-*J* experiment, J. Magn. Reson. 146 (2000) 255–259.

[22] P. Permi, Measurement of residual dipolar couplings from $^{1}H^{\alpha}$ to $^{13}C^{\alpha}$ and ^{15}N using a simple HNCA-based experiment, J. Biomol. NMR 27 (2003) 341–349.

[23] E. Miclet, J. Boisbouvier, A. Bax, Measurement of eight scalar and dipolar couplings for methine-methylene pairs in proteins and nucleic acids, J. Biomol. NMR 31 (2005) 201–216.

[24] J.R. Garbow, D.P. Weitekamp, A. Pines, Bilinear rotation decoupling of homonuclear scalar interactions, Chem. Phys. Lett. 93 (1993) 504–509.

[25] D. Uhrín, T. Liptaj, K.E. Kövér, Modified BIRD pulses and design of heteronuclear pulse sequences, J. Magn. Reson. Ser. A 101 (1993) 41–46.

[26] T.L. Hwang, A.J. Shaka, Water suppression that works. Excitation sculpting using arbitrary wave-forms and pulsed-field gradients, J. Magn. Reson. 112A (1995) 275–279.

[27] M.R. Hansen, L. Mueller, A. Pardi, Tunable alignment of macromolecules by filamentous phage yields dipolar coupling interactions, Nat. Struct. Biol. 12 (1998) 1065–1074.
[28] W.F. Vranken, W. Boucher, T.J. Stevens, R.H. Fogh, A. Pajon, E. Ulrich, M. Llinas, J. Ionides, E.D. Laue, The CCPN data model for NMR spectroscopy: development of a software pipeline, Proteins 59 (2005) 687–696.
[29] P. Permi, S. Heikkinen, I. Kilpeläinen, A. Annila, Measurement of $^{1}J_{NC'}$ and $^{2}J_{HNC'}$ couplings from spin-state-selective two-dimensional correlation spectrum, J. Magn. Reson. 140 (1999) 32–40.
[30] L. Emsley, G. Bodenhausen, Gaussian pulse cascades: new analytical functions for rectangular selective inversion and in-phase excitation in NMR, Chem. Phys. Lett. 165 (1990) 469–476.
[31] P. Jensen, H.-J. Sass, S. Grzesiek, Improved detection of long-range residual dipolar couplings in weakly aligned samples by Lee-Goldburg decoupling of homonuclear dipolar truncation, J. Biomol. 30 (2004) 443–450.
[32] K. Fehér, S. Berger, K.E. Kövér, Accurate determination of small one-bond heteronuclear residual dipolar couplings by *F*1 coupled HSQC modified with a G-BIRD$^{(r)}$ module, J. Magn. Reson. 163 (2003) 340–346.
[33] K.E. Kövér, G. Batta, More line narrowing in TROSY by decoupling of long-range couplings: shift correlation and $^{1}J_{NC'}$ coupling constant measurements, J. Magn. Reson. 170 (2004) 184–190.
[34] T.N. Pham, T. Liptaj, K. Bromek, D. Uhrín, Measurement of small one-bond proton–carbon residual dipolar coupling constants in partially oriented ^{13}C natural abundance oligosaccharide samples: analysis of heteronuclear $^{1}J_{CH}$-modulated spectra with the BIRD inversion pulse, J. Magn. Reson. 157 (2002) 200–209.
[35] J. Keeler, Understanding NMR Spectroscopy, Wiley, 2005.
[36] G. Kontaxis, G.M. Clore, A. Bax, Evaluation of cross-correlation effects and measurement of one-bond couplings in proteins with short transverse relaxation times, J. Magn. Reson. 143 (2000) 184–196.
[37] L.E. Kay, M. Ikura, R. Tschudin, A. Bax, Three-dimensional triple-resonance NMR spectroscopy of isotopically enriched proteins, J. Magn. Reson. 89 (1990) 496–514.